Carbonyl sulfide in the planetary boundary layer: Coastal and continental influences

R. Commane,[1] S. C. Herndon,[2] M. S. Zahniser,[2] B. M. Lerner,[3] J. B. McManus,[2] J. W. Munger,[1] D. D. Nelson,[2] and S. C. Wofsy[1]

Received 31 January 2013; revised 10 June 2013; accepted 14 June 2013.

[1] Measurements of carbonyl sulfide (OCS) have been proposed to provide a unique constraint on carbon assimilation by the biosphere that is independent of the influence of plant and soil respiration of CO_2, but this constraint depends on a comprehensive understanding of the processes controlling OCS in the biosphere. We conducted a high-resolution temporal and spatial survey of OCS and CO_2 mixing ratios during the California Nexus Experiment research cruise along the coast of California (U.S.) and into the Sacramento River Delta using a newly constructed compact quantum cascade laser spectrometer (precision for OCS of <8 pptv (pmol/mol) at 1 Hz). The temporal and spatial resolution of the measurements revealed a number of specific processes related to known sources and sinks. The observations demonstrate OCS uptake during daytime photosynthetic uptake of CO_2, OCS depletion during nighttime forest respiration of CO_2, and OCS emission from a freshwater marsh. OCS emission was observed in one anthropogenically influenced plume, but, overall, no correlation was observed between OCS and SO_2, and the use of scaled SO_2 emission fields in global budgets of OCS should be reconsidered for areas with strict sulfur emission controls, such as California. The observations show that, in a homogeneous ecosystem on a local scale, OCS may be a proxy for CO_2 uptake. However, at larger scales that span heterogeneous environments, in order to confidently quantify any single process, competing processes must be either relatively small or well quantified.

Citation: Commane, R., S. C. Herndon, M. S. Zahniser, B. M. Lerner, J. B. McManus, J. W. Munger, D. D. Nelson, and S. C. Wofsy (2013), Carbonyl sulfide in the planetary boundary layer: Coastal and continental influences, *J. Geophys. Res. Atmos.*, *118*, doi:10.1002/jgrd.50581.

1. Introduction

[2] Measurements of atmospheric carbonyl sulfide (OCS) concentrations have been suggested as a means to constrain carbon assimilation in the biosphere, without the need for prior knowledge of plant and soil respiration [*Sandoval-Soto et al.*, 2005; *Campbell et al.*, 2008; *Blonquist et al.*, 2011]. However, this constraint depends on our understanding of the processes in the biosphere that control OCS in the atmosphere and its relationship with CO_2. Most studies to determine OCS and CO_2 behavior have either scaled up soil or leaf chamber studies to the ecosystem scale, with some significant assumptions [e.g., *Seibt et al.*, 2010; *Stimler et al.*, 2010], or used widely dispersed measurements to try to understand processes on the regional and continental scales [e.g., *Montzka et al.*, 2007; *Campbell et al.*, 2008]. There are limited studies that focus on the ecosystem-scale processes in the field [e.g., *Mihalopoulos and Nguyen*, 2001; *Xu et al.*, 2002; *Asaf et al.*, 2013], and the need for the development of instruments of high temporal sensitivity has been previously highlighted [*Blonquist et al.*, 2011].

[3] OCS is the most abundant sulfur-containing gas in the atmosphere, with mixing ratios varying between 300 pptv (parts per trillion = pmol mol^{-1}) and 550 pptv at background sites around the globe, and these current annual global concentrations show little trend, indicating that a balance exists between OCS sources and sinks [*Montzka et al.*, 2007]. Global budgets indicate that about half the OCS in the atmosphere is the result of direct and indirect emission from oceans [*Watts*, 2000; *Kettle*, 2002; *Suntharalingam et al.*, 2008], with the balance from wetlands, biomass burning, and industry [*Watts*, 2000; *Blake et al.*, 2004]. OCS is directly emitted from the ocean in areas of high productivity [e.g., *Kettle et al.*, 2001; *Xu et al.*, 2001]. Indirect emissions of OCS arise from the oxidation of dimethylsulfide (DMS) and carbon disulfide (CS_2) [*Barnes et al.*, 1994, 1996], with fluxes of OCS from these sources comparable to the direct oceanic flux [*Kettle*, 2002].

[1]School of Engineering and Applied Sciences, Harvard University, Cambridge, Massachusetts, USA.
[2]Aerodyne Research Inc., Billerica, Massachusetts, USA.
[3]NOAA Earth System Sciences Research Laboratory, Boulder, Colorado, USA.

Corresponding author: R. Commane, School of Engineering and Applied Sciences, Harvard University, Cambridge, MA 02138, USA. (rcommane@seas.harvard.edu)

2169-897X/13/10.1002/jgrd.50581

[4] Removal of OCS is dominated by uptake in the terrestrial biosphere, with vegetative uptake of OCS much greater than uptake by soils. The combined uptake by plants and soils is more than 3 times greater than the destruction of OCS through tropospheric oxidation and stratospheric photolysis [*Chin and Davis*, 1995; *Watts*, 2000]. The biological pathways by which leaves consume OCS and CO_2 are initially complementary, before following distinct pathways. Carbonic anhydrase (CA) catalyzes the hydrolysis of OCS to produce H_2S and CO_2 in an essentially irreversible reaction [*Protoschill-Krebs et al*., 1996; *Schenk and Kesselmeier*, 2004]:

$$OCS + H_2O \xleftrightarrow{CA} HCOOS^- + H^+ \longleftrightarrow H_2S + CO_2$$

[5] CA also reversibly catalyzes CO_2 hydrolysis before the CO_2 goes on to react with light activated enzymes (e.g., RuBisCo). Therefore, although OCS is taken up by plants during photosynthesis, unlike CO_2, it is not emitted during respiration. Laboratory studies have shown the OCS/CO_2 uptake rate varies around 1.6 ± 0.26 pptv ppmv^{-1} for a range of vegetative species, with trees (1.7 ± 0.9 pptv ppmv^{-1}) assimilating relatively more OCS than shrubs (1.2 ± 0.1 pptv ppmv^{-1}) [*Stimler et al*., 2012]. On the ecosystem scale, measurements of OCS and CO_2 have shown a relative uptake of 2.9 (±1.8) for crops and arid pine forests, reflecting the sources of CO_2 respiration on the ecosystem scale [*Asaf et al*., 2013]. A study of seasonal uptake on a continental scale found that relative OCS uptake was 5–6 times larger than CO_2 uptake [*Montzka et al*., 2007; *Asaf et al*., 2013], which may be due to additional anthropogenic sources of CO_2 on the continental scale. While the loss of OCS in the biosphere is dominated by vegetation, OCS also interacts with soils, where emission or uptake depends on the soil composition, and is also mediated by carbonic anhydrase. Some previous soil emission experiments were found to be compromised by unsuitable analytical measurement techniques (as highlighted by *Castro and Galloway* [1991]). However, more recent studies have found that oxic and anoxic soils are sinks and sources of OCS, respectively [e.g., *Kesselmeier et al*., 1999; *Kuhn et al*., 1999; *Simmons et al*., 1999; *Steinbacher et al*., 2004; *Yi et al*., 2007; *Liu et al*., 2010].

[6] Recently, ecosystem flux measurements of OCS have been made by *Asaf et al*. [2013] using an instrument similar (but with some distinct differences) to that used here (and described by *Stimler et al*. [2009]). However, most other previous measurements of OCS have been made by discontinuous, low-frequency techniques. Flask samples collected at remote field sites or on aircraft have provided a valuable long-term and spatially widespread record of OCS [e.g., *Blake et al*., 2004; *Montzka et al*., 2007; *Blake et al*., 2008; *Campbell et al*., 2008; *de Gouw et al*., 2009]. For example, within the National Oceanic and Atmospheric Administration (NOAA) network, flasks are analyzed in a laboratory using gas chromatography coupled to mass spectrometry [e.g., *Montzka et al*., 2004] with excellent precision and accuracy. However, while the spatial distribution of these measurements describe regional- and continental-scale processes, the sampling frequency at field sites in this network is typically weekly or once every 2 weeks, so diel processes cannot be investigated [*Blonquist et al*., 2011].

[7] We have developed a high-frequency, continuous measurement technique, with simultaneous measurement of CO_2 in the same instrument (section 2) that greatly enhances our capability to study how OCS is related to the emission and uptake processes of CO_2. Measurements of OCS and CO_2 mixing ratios were made along the coast of California and up the Sacramento River Delta as part of the California Nexus Experiment (CalNex) campaign in May/June 2010. The observations highlighted the range of influences on the OCS/CO_2 ratio that were evident, including OCS depletion during the photosynthetic uptake of CO_2 (section 3.2.1), nighttime emission of OCS from a wetland coincident with CO_2 respiration (section 3.2.2), and depletion of OCS during respiration of CO_2 from a redwood forest (section 3.2.3). Large anthropogenic emissions of OCS were observed from a single source in the Los Angeles basin (section 3.3). A large-scale increase in mean OCS was also observed during the cruise with the arrival of clean marine air (section 3.4).

2. Instrumentation

[8] A Tunable mid-Infrared Laser Direct-Absorption Spectrometer (TILDAS) using continuous-wave quantum cascade lasers (QCLS) was built at Aerodyne Research Inc. (Billerica, MA, USA) and deployed aboard the R/V *Atlantis* during the California Nexus Experiment (CalNex) research cruise along the coast of California from San Diego to Sacramento between 15 May and 8 June 2010. The instrument was operated with a configuration allowing for two lasers: measurements of OCS and CO_2 (made at 2052.256 cm^{-1} and 2052.096 cm^{-1}, respectively) were coupled with measurements of formaldehyde (HCHO) and formic acid (HCOOH) from the second laser at 1765 cm^{-1}. Details of the optics, multipass cell, and overall instrument layout are described in *McManus et al*. [2010, 2011]. A continuous-wave quantum cascade laser (Alpes Lasers, *Faist et al*. [1994]) was maintained at low temperature (~0.7°C) in a hermetically sealed enclosure by a Peltier element coupled to a recirculating Thermocube chiller. Current to the laser was supplied by a high-compliance source (QCL-7B, Wavelength Electronics, Inc.) with current modulation input determined by the D-A output of the computer. Each laser was scanned sequentially across 400 channels at ~0.002 cm^{-1}/channel with complete spectra acquired at a frequency of 1.1 kHz. For an additional 36 channels at the end of each scan, the laser currents were both reduced to below the lasing threshold to measure the detector "zero light" signal. The ramped laser current generates a slightly nonlinear laser tuning rate, which was determined by fitting the spectrum of a germanium etalon.

[9] The laser light was directed into an astigmatic Herriot style multipass absorption cell operated at low pressure (38 Torr). An effective path length of 200.1 m was achieved with 422 passes between high-reflective coated mirrors placed 47.42 cm apart. The laser light exiting the multipass cell was directed to a liquid nitrogen cooled HgCdTe detector. Mixing ratios of OCS and CO_2 at a frequency of 1 Hz were calculated using the TDL Wintel software (Aerodyne Research Inc.). Background spectra averaged for 14 s were acquired every 2 min in order to account for any changes in instrument response with time. The sample spectra were normalized by dividing by the background spectra

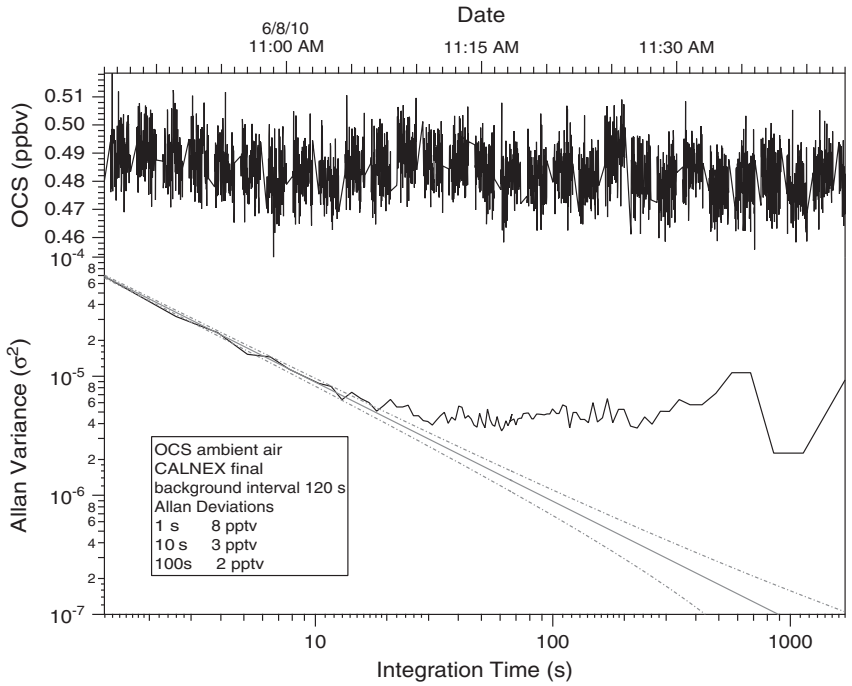

Figure 1. Allan variance plot of instrumental performance at the end of the campaign. The instrument showed a 1 s precision of 8 pptv averaging down to 2 pptv at 50 s.

interpolated in time [*Nelson et al*., 2004]. A flow rate of 10 standard liters per minute through the 2 L cell at 38 Torr resulted in a cell response time of 0.6 s. Details of the laser control system, sampling cell, detectors, data acquisition, and spectral fitting software have been described previously in *McManus et al*. [2010, 2011].

[10] During the CalNex cruise aboard the R/V *Atlantis*, an 18 m tower on the starboard foredeck allowed for sampling OCS and CO_2 ~28 m from the sea surface. A custom-built glass inlet with a virtual impactor directed large particles (>200 nm diameter) into a bypass flow, which eliminated the need for a filter at the inlet to protect the sample line and high reflectivity sample cell mirrors from large particles. An OCS standard was periodically introduced to the sampling inlet, and the instrument response to this standard varied by 3.8% (358 ± 13 pptv, 1σ) during the cruise, without any systematic temporal trend. The instrument precision throughout the measurement period was 8 pptv (1 s) averaging down to 2 pptv at 50 s (Figure 1 is an Allan variance plot of the precision of the instrument). The absolute spectroscopic accuracy, determined from standard gas additions, was ~5% of the total OCS (~20 pptv).

[11] The instrument has improved sensitivity compared to an earlier generation quantum cascade laser spectrometer [*Stimler et al*., 2009] (8 pptv s^{-1} versus 50 pptv s^{-1}), in part due to the use of a continuous wave (cw) rather than a pulsed laser. The cw laser has sharper line width, producing deeper absorption peaks, and reproducible laser output power. The cw laser stability is sufficient to eliminate the need for a normalization beam path, which is necessary in pulsed mode. Finally, the multipass cell in the current instrument has a 200.1 m path compared to 76 m for the cell used by *Stimler et al*. [2009].

[12] Inlets for carbon monoxide (CO) and carbon dioxide (CO_2) (operated by B. M. Lerner, NOAA) were co-located on the tower allowing for direct comparison with OCS observations. CO was measured using an Aerolaser AL5002 vacuum-UV fluorescence detector with 1.6 ppbv (1 s) precisions averaged down to 0.5 ppbv at 1 min, and 4% accuracy. CO_2 was measured using a LI-COR 7000 nondispersive IR absorption detector with 0.08 ppmv (1 s) precision averaged down to 0.04 ppmv at 1 min, and 0.15 ppmv accuracy. For both measurements, ambient water vapor is removed (to less than 1 ppth (parts-per-thousand, equivalent to mmol mol-1)) from the sample stream by a Nafion drier before analysis, as the CO instrument has a minor water sensitivity. Mixing ratios are reported as measured in dry air. Both instruments were calibrated periodically throughout the cruise with standard gases. A comparison of the LI-COR calibrated CO_2 and the uncalibrated CO_2 reported by the QCLS instrument found that the QCLS CO_2 consistently underestimated CO_2 by 5%. The three-point CO_2 calibration of the LI-COR was traceable to primary standards maintained by NOAA GMD (Global Monitoring Division); therefore, the LI-COR CO_2 data were used for analysis, except for 1 Hz OCS/CO_2 comparisons (section 3.2.2) where the QCLS CO_2 data were linearly scaled by 1.05 to match the GMD scale.

[13] The photolysis rate of formaldehyde (jHCHO, $\lambda > 330$ nm), calculated from a diffused filtered radiometer (B. M. Lerner, NOAA) co-located with the inlet, is presented here as a proxy for solar radiation. Photolysis rates follow the timing of sunrise and sunset and extent of attenuation by cloud cover.

3. Results and Discussion

[14] In order to study the major processes controlling the OCS relationship with CO_2, mixing ratios of OCS and CO_2 in air of both continental and marine origin were sampled along the coast of California aboard the R/V *Atlantis* during the CalNex cruise in May/June 2010 [*Ryerson et al*., 2013].

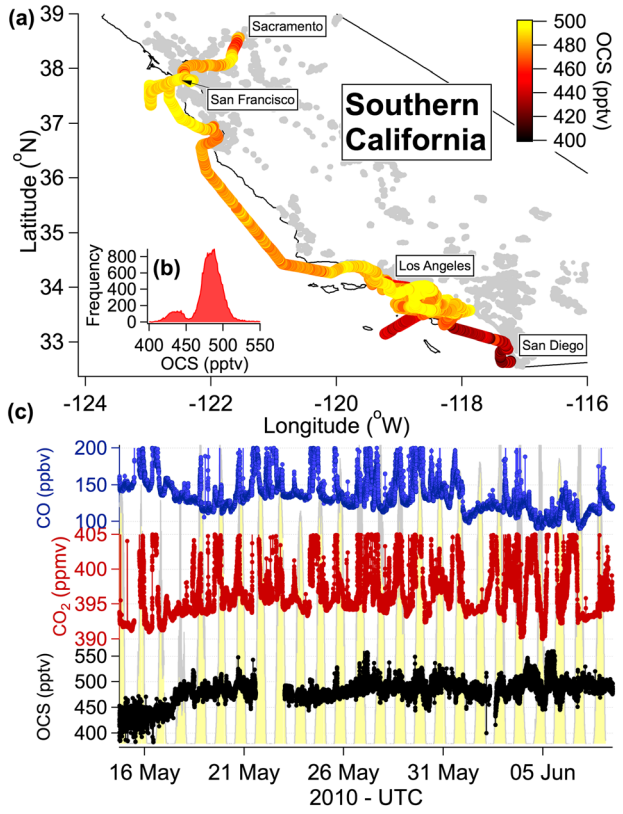

Figure 2. (a) OCS mixing ratios observed along the coast of California from San Diego to San Francisco in May/June 2010 aboard the R/V *Atlantis*. Areas of urban populations are indicated in gray (data provided by the California Air Resource Board). OCS ranged from 385 pptv to over 2 ppbv on rare occasions. (b) Histogram of OCS mixing ratios (1 pptv mixing ratio bins). Two distinct populations were evident: Initial mixing ratios centered around 436 pptv, increasing to 480 pptv after the arrival of marine-influenced and processed air into the region. The source of this change is discussed in section 3.4. (c) Mixing ratios of CO (blue squares), CO_2 (red diamonds) and OCS (black circles) plotted in UTC. Plots have been truncated to highlight mixing ratios closer to background levels (CO < 200 ppb and CO_2 < 405 ppmv). The regions sampled include (i) LA Basin (15 May to 1 June), (ii) coastal region (1–2 June), and (iii) bay area and Sacramento River Delta (3–8 June). The observed photolysis rate of jHCHO is shown in yellow behind the mixing ratios to indicate daylight.

The observations highlight a range of influences on the OCS/CO_2 ratio that are examined in detail below.

3.1. Cruise Track

[15] Figure 2(a) outlines the OCS mixing ratios observed along the cruise track. Starting in San Diego on 15 May, the ship spent several days offshore of the Los Angeles Basin sampling air mainly influenced by continental and urban emissions. On 1 June, the ship traveled from Ventura to Monterrey Bay, sampling a mix of continental and marine air. The ship sampled a land breeze overnight in Monterrey Bay before continuing north, sampling open ocean air, and into San Francisco Bay. From 3 to 8 June, the ship traveled through the Sacramento River Delta via the Sacramento River Deep Water Ship Channel, surrounded by agricultural areas, before returning to port in San Francisco. Figure 2(c) shows the time series of CO, CO_2, and OCS throughout the cruise with jHCHO used to indicate daylight (time in UTC).

3.2. Biogenic Processes Related to OCS

[16] Figure 3 highlights a time period when the ship was located in the Sacramento River Delta (4/5 June), ~160 km up the Sacramento River Deep Water Ship Channel from the Pacific ocean. The OCS-CO_2 relationship showed evidence of OCS loss during the daytime photosynthetic uptake of CO_2 (discussed in detail in section 3.2.1) and OCS emission during the nighttime respiration of CO_2 (discussed in detail in section 3.2.2)

3.2.1. Depletion of OCS During Photosynthesis

[17] In the Sacramento River Delta, sampled air (Figure 3; 4 June) traveled over the Yolo Bypass Wildlife area, a 65 km^2 wildlife preserve located to the west of Sacramento, with limited anthropogenic gas emission before sampling. The eastern and southern borders of the area are defined by the Sacramento Deep Water Ship Channel, and the area contains a large fraction of rice paddies, which were subject to controlled flooding for rice planting about 2 months previously.

[18] Variations in mixing ratio are influenced both by mixing between different air masses, such as ventilation of the surface boundary layer and inland penetration of marine air, and the accumulated depletion/enhancement of species due to surface exchange. During the period shown in Figure 4 (21:00 on 4 June to 03:00 on 5 June), we observe a simultaneous depletion of OCS and CO_2 in air masses that came from the Pacific Ocean and passed over agricultural areas in the previous 24 h (HYSPLIT Trajectory calculations

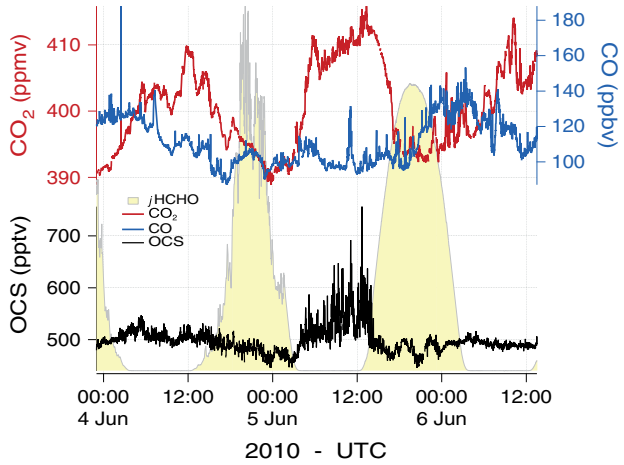

Figure 3. Time Series of CO_2 (red), CO (blue), OCS (black) and the photolysis rate of formaldehyde (jHCHO, used as a proxy for daylight) (yellow) around Sacramento. The influence of photosynthetic uptake of OCS and CO_2 was seen as parallel decline in OCS and CO_2 on 4 June (up to 02:00 UTC on 5 June). Then both increased due to strong local emissions of OCS and CO_2 from a nearby wetland, overnight on 5 June. On this night, wind speeds varied between 1 and 4 m s^{-1}. No OCS increase was associated with increasing CO when sampling downwind of a petrochemical refinery (6 June).

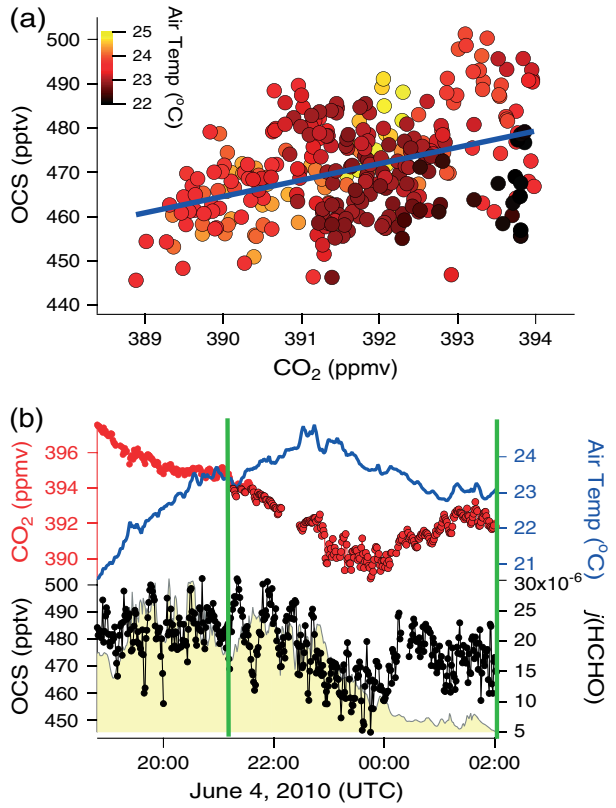

Figure 4. (a) OCS (pptv) versus CO_2 (ppmv) for afternoon air on 21:00 UTC on 4 June to 03:00 UTC on 5 June 2010 in Sacramento with a signature of photosynthetic uptake: +3.7 (±0.5) pptv OCS/ppmv CO_2. (b) Time series of OCS (black), CO_2 (red), air temperature (blue) and formaldehyde photolysis rate (yellow). OCS and CO_2 both decrease with increasing-temperature through the day but reach a minimum in the hour after the highest temperature, which is likely a function of the airmass transport time. Data between the green lines is used in Figure 4(a).

using reanalysis data; *Draxler and Rolph* [2012]). In clean marine boundary layer air sampled offshore to the west of San Francisco 48 h before and 72 h after this measurement period, we observe a clean air baseline of 494 (±8) pptv OCS and 393.83 (±0.15) ppmv CO_2. During this event, both CO_2 and OCS were below the MBL (marine boundary layer) baseline, indicating ventilation by clean air could not have accounted for the observed trend by itself. We derive a signal for uptake associated with vegetation activity by looking at covariance of CO_2 and OCS in the samples that had mixing ratios of OCS and CO_2 below the clean marine baseline.

[19] Figure 4(a) shows that in photosynthetically influenced air sampled in the Sacramento River Delta, OCS was correlated with CO_2, with 3.7 (±0.5) pptv of OCS lost for each ppmv of CO_2 taken up during photosynthesis, indicating that the vegetation growing through the flooded fields in June acts as a sink of both OCS and CO_2. Previous studies have shown that, while rice paddies act as a source of OCS when initially flooded, water-logged rice paddies with visible vegetation act as a sink of OCS [*Yi et al.*, 2008; *Liu et al.*, 2010]. Both OCS and CO_2 mixing ratios decrease with warming air temperatures (Figure 4(b)). The minimum mixing ratios were observed approximately 1 h after the maximum air temperature, before increasing again as the temperature cools. Shipboard temperatures (measured at the OCS sampling height) are not a measure of the temperature at the point of OCS and CO_2 uptake. Therefore, it is not possible to distinguish whether the timing of OCS and CO_2 minima is coincidence of transport or evidence for temperature dependence of OCS and CO_2 uptake. Similarly, photosynthetically active radiation (PAR) is closely linked with air temperature and is a strong driver of photosynthesis on a diel scale so PAR may be influencing the OCS/CO_2 ratio. Above agricultural fields, *Prueger et al.* [2004] found CO_2 mixing ratios decreased throughout the day alongside substantial CO_2 uptake, in a manner similar to that seen in Figure 4. The OCS/CO_2 ratio of 3.7 pptv/ppmv observed here is the net effect of both photosynthesis and respiration components of CO_2 and is within the range of the ecosystem-scale relative uptake of 2.9 (±1.8) measured by *Asaf et al.* [2013] for a range of crop and arid pine forests using eddy covariance.

3.2.2. Natural Wetland Emission of OCS

[20] Figure 3 shows relatively rapid variations in both OCS and CO_2 during the night of 5 June, while the ship was located in the Sacramento Turning Basin, ~160 km from the coast. The mixing ratios of both OCS and CO_2 accumulate throughout the night, first increasing as night falls and the nocturnal boundary layer stabilizes. A detailed examination of 30 min of data during this period (Figure 5) showed that enhanced OCS (between 500 pptv and 700 pptv) was strongly correlated with short-term increases in CO_2

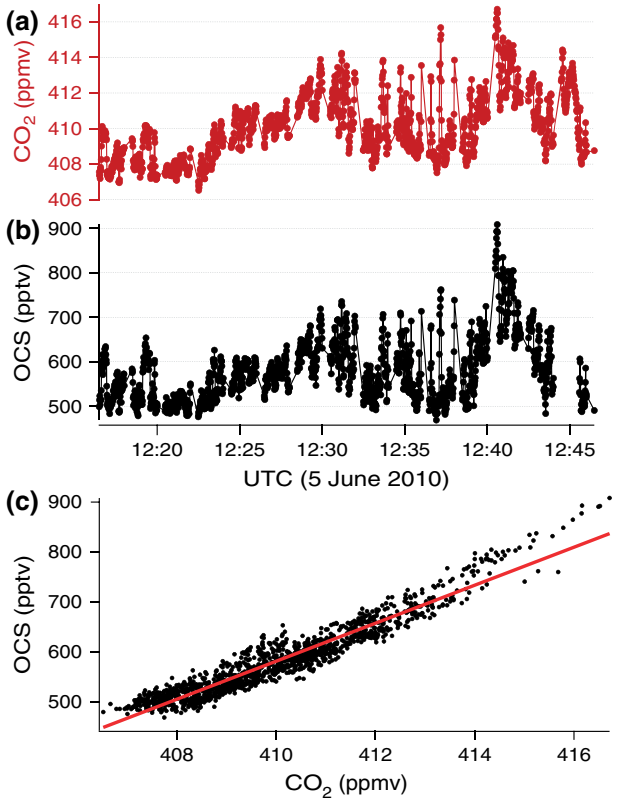

Figure 5. The 1 Hz OCS and CO_2 observed for 30 min close to dawn on 5 June 2010. OCS emission and CO_2 respiration were strongly correlated (r = 0.95) with a slope of 38 pptv/ppmv, indicating a colocated source.

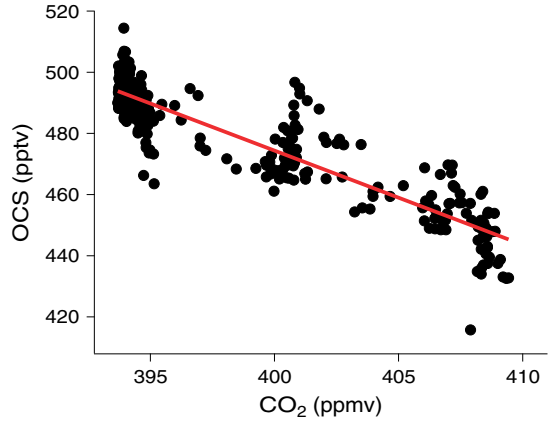

Figure 6. Nocturnal depletion of OCS during CO_2 respiration observed in the continental outflow in Monterrey Bay on 1 June 2010. OCS at 3.1 (±0.1) pptv was lost for every ppmv of CO_2 respired.

(between 400 and 415 ppmv), and up to 38 pptv OCS was emitted for every ppmv of CO_2 (Figure 5(c), r = 0.95, sampling frequency of 1 Hz). Variability of both OCS and CO_2 was extremely rapid and tightly coupled, which was made evident by the simultaneous measurement of both species in the same instrument. The tight correlation of OCS and CO_2 evident in this 1 s data (r = 0.95) suggests a nearby common source of OCS and CO_2, with high-frequency variability generated by vagaries in transport and dilution. Lower frequency observations of OCS and CO_2 would not have identified this source. Lake Washington, a shallow freshwater lake with substantial marshy edges during the summer months, was ~100 m to the south and upwind of the ship, which was docked in the Turning Basin, during the periods of high OCS. *Whelan et al*. [2013] found a comparable ratio of ~36 pptv OCS emitted for each ppmv of CO_2 respired for a range of saltwater marshes. Previous studies of freshwater marshes suggest that marshes are a source of OCS (around 7 pptv m^{-2} s^{-1}; *Hines et al*. [1993]). However, this study used sulfur-free air as a carrier gas for chamber studies, possibly leading to artificial OCS emission [*Watts*, 2000]. The observations here support the inference that marshes can be a significant dark source of OCS, and emission of OCS from anoxic soils has been underestimated [*Whelan et al*., 2013]. However, it is also possible that OCS is released coincidently with the respiration of CO_2 from vegetation in or surrounding Lake Washington. Within 2 h of first light the following morning, the wind direction changed to bring air from over the Yolo Wildlife area again, and both CO_2 and OCS returned to background levels.

3.2.3. Depletion of OCS at Night

[21] Depletion of OCS was observed in stable nocturnal boundary layer air influenced by CO_2 respiration. Respiration by vegetation, roots, and soils emits CO_2, which accumulates in the nocturnal boundary layer. Depletion of OCS, coincident with CO_2 accumulation, was observed in the outflow from the north of Monterrey Bay overnight and towards dawn on 1 June 2010, when the ship was between 1.6 and 4 km offshore. Figure 6 shows an inverse OCS to CO_2 correlation, where 3.1 (±0.1) pptv of OCS was lost for every ppmv of CO_2 emitted (r = 0.91). Radon levels were elevated in line with a terrestrial influence, and there was no enhancement in marine tracer species such as dimethyl sulfide. At the end of the night, OCS increased and CO_2 decreased with the breakup of the nocturnal boundary layer and entrainment of free tropospheric air. Back trajectories (HYSPLIT Trajectory calculations using reanalysis data; *Draxler and Rolph* [2012]) for this period indicate that the air had passed over extended redwood forests and bare soils, suggesting an ecosystem-scale nocturnal uptake of OCS. These offshore measurements were too far away to distinguish between uptake in the soil or through stomata that remain partially open at night [*Caird et al*., 2006; *Daley and Phillips*, 2006]. Without more knowledge of the nocturnal boundary layer height and stability along the trajectory, the fluxes of OCS into and CO_2 out of the ecosystem cannot be quantified. However, the OCS and CO_2 mixing ratios are equally affected by the mixing layer height allowing us to interpret the OCS/CO_2 ratio as the relative rate of OCS uptake associated with nighttime respiration of CO_2.

[22] Previous studies of OCS interaction with soil have shown a large range of uptake and emission rates, depending on soil type. Unlike the emission seen in anoxic soils and marshes (e.g., section 3.2.2 above, *Yi et al*. [2008], *Whelan et al*. [2013]), oxic soils are generally a sink of OCS [e.g., *Kesselmeier et al*., 1999; *Simmons et al*., 1999; *Conrad and Meuser*, 2000; *Steinbacher et al*., 2004; *Van Diest and Kesselmeier*, 2008]. In those studies, the uptake of OCS by soils was regulated by soil moisture and temperature.

3.3. Anthropogenic Emission of OCS

[23] Direct anthropogenic emission is a source of OCS [e.g., *Chin and Davis*, 1995; *Blake et al*., 2008]. Unlike CO and CO_2, which showed large enhancements, there were no OCS enhancements when sampling the engine exhaust of the R/V *Atlantis*, which was burning ultralow sulfur fuel throughout the cruise. Only one anthropogenic pollution plume with high OCS was observed, when up to 2 ppbv OCS was sampled in air, which had passed over a 20 acre liquidized petroleum gas (LPG) storage facility and refinery in the port of Los Angeles on 27 May. The ship was docked less than 100 m downwind of the facility. Winds from the north and northwest sectors passed over the facility and reached the ship in less than a minute, with wind speeds of between 2 and 5 m s^{-1}. OCS emission from the facility continued throughout a 5 h period, but no emission of OCS was detected after a change of wind direction at 5 A.M. UTC (8 P.M. local time). OCS was not highly correlated with typical tracers of anthropogenic combustion, such as CO, CO_2, NO_x, acetonitrile, etc. but rather showed evidence of independent short-lived events with a partially oxidized sulfur contribution, e.g., the addition of odorant to the gas. OCS and SO_2 were weakly correlated for a time when sampling the plume from the facility (38 ppt/ppb, r = 0.52), but the largest increases in SO_2 mixing ratios were not matched by increases in OCS mixing ratios. OCS mixing ratios were over twice the largest mixing ratio observed from wetland emissions (section 3.2.2).

[24] Mixing ratios of OCS at ppmv levels can be produced in the desulfurization of fuel and in the sulfur recovery process in LPG processing [*Svoronos and Bruno*, 2002], but OCS was not emitted from all gas/petrochemical facilities sampled. No OCS emissions were observed from a

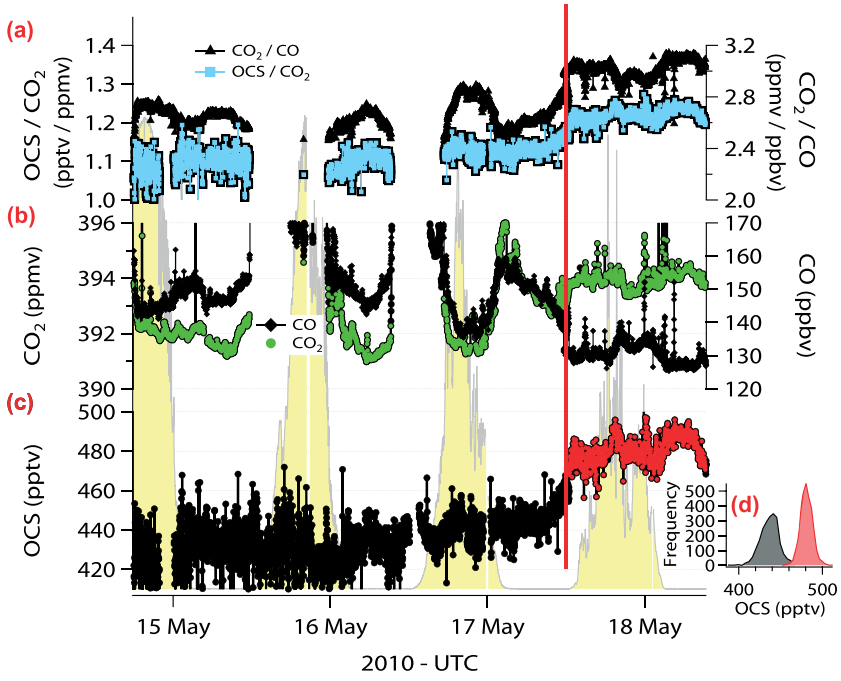

Figure 7. A change of airmass on 17 May (red line) led to (a) an increase in the CO_2/CO ratio (black) and OCS/ CO_2 ratio (blue), (b) a decrease in CO (black) and increase in minimum CO_2 (green), and (c) an increase in OCS of 50 pptv. (d) Histogram of OCS data before (black, 15–17 May) and after (red, 17–19 May) shows the increase in mixing ratio (from 436 to 480 pptv) and the reduction in variability of OCS (11 pptv to 7 pptv) evident after the airmass change.

petrochemical refinery located on the Sacramento River on the night of 6 June (as shown in the time series presented in Figure 3), although CO, CO_2, and SO_2 mixing ratios were all enhanced, with SO_2 reaching up to 10 ppbv. This suggests that OCS emission from anthropogenic sources is associated with very specific applications rather than being a widespread observation.

[25] Global budgets of OCS use scaled SO_2 emission fields to distribute the global OCS anthropogenic emission [e.g., *Kettle*, 2002; *Suntharalingam et al.*, 2008]. However, no correlation was found between OCS and SO_2 for the total data series observed here, suggesting that the use of SO_2 emission fields may not be suitable for areas where low sulfur fuels use is extensive, such as California. The relationship between OCS and SO_2 should be investigated further with fast response instrument (such as the spectroscopic instrument described here) to determine how well the distribution of OCS anthropogenic emissions matches SO_2 anthropogenic emissions in both stack/point emissions and on a wider scale.

3.4. Airmass Origin: Long-Range Transport

[26] OCS mixing ratios observed early in the cruise (May 2010) highlight how clean marine air contains ~10% more OCS than continental air. Two distinct populations of OCS mixing ratios, centered at 436 and 480 pptv, are evident in histogram of the observations (Figures 2(b) and 7(d)). This step change in OCS mixing ratios occurred over a few hours on 17 May and is related to a large-scale change of airmass at 12:30 UTC 17 May (Figure 7). Back-trajectory calculations (HYSPLIT) show that the sampled air changed from continental influenced air recirculating within the LA Basin and nearshore waters to clean marine air. Figure 7 shows the OCS, CO_2, and CO time series and the CO_2/CO and OCS/CO_2 ratios. From 15 to 17 May, OCS mixing ratios were centered around 436 (±11) pptv (1σ) before, within a matter of hours, increasing to 480 (± 7) pptv (1σ) and were not significantly depleted during the remainder of the campaign (Figure 7(c)). In this marine air, the air temperature dropped from 13.2°C to 10.8°C, and the relative humidity increased from 90% to 99%. Minimum CO_2 increased from 391 ppmv to 393 ppmv, and CO decreased from 150 ppbv to 130 ppbv (Figure 7(b)). A decreased CO/CO_2 ratio indicates a greater oxidation of trace gases in the marine airmass, and a decreased variance in OCS suggests that this marine air had passed over a region of homogeneous or limited sources or sinks of OCS. A short-lived increase was seen in dimethylsulfide (DMS), which has a marine source and is thought to be a source of OCS [*Barnes et al.*, 1994, 1996]. Conversely, CO, NO_2, O_3, and radon, all of which have terrestrial/anthropogenic sources, were lower in the clean marine air.

4. Conclusions

[27] The ecosystem-scale relationship of OCS and CO_2 may provide a means to determine the photosynthetic uptake of CO_2. In order to examine this relationship on a fine scale, we developed an infrared quantum cascade laser absorption analyser with precision for OCS at 1 Hz of better than 8 pptv (pmol/mol). High-frequency (1 Hz) simultaneous measurements of OCS and CO_2 mixing ratios were made in air sampled along the coast of California and into the Sacramento River Delta during the CalNex cruise aboard the R/V *Atlantis* in May/June 2010.

[28] The high spatial and temporal resolution of these observations allowed for the identification of a number of OCS/CO_2 processes. OCS depletion during the photosynthetic uptake of CO_2 was observed in air traveling over rice paddies along the Sacramento River (3.7 (±0.5) pptv OCS /ppmv CO_2). This is comparable to the ecosystem relative uptake of OCS/CO_2 of 2.9 (±1.8) observed by *Asaf et al*. [2013]. Wetland emission of OCS was observed at night during respiration from a freshwater lake (38 pptv OCS /ppmv CO_2), a much larger emission than observed previously. Ecosystem-scale deposition of OCS at night was observed in air passing over a redwood forest (−3 pptv OCS/ppmv CO_2). This may be due to uptake by soils or incompletely closed stomata, but further elucidation is not possible with the current measurements. Short-lived anthropogenic emissions up to 2 ppbv weakly correlated with SO_2 emission were observed when sampling air from a liquid petroleum gas refinery. However, OCS was not correlated with SO_2 at other petrochemical sites, and the use of scaled SO_2 emission fields as a proxy for OCS anthropogenic emission in global models should be reconsidered. Clean marine air was found to contain ~10% more OCS than continentally influenced air during May/June, which is consistent with marine sources and terrestrial sinks. These observations show that, in a homogeneous ecosystem on a local scale, OCS may be a proxy for CO_2 uptake. However, at larger scales that span heterogeneous environments, competing processes must be either relatively small or well quantified in order to confidently quantify any single process.

[29] **Acknowledgments.** We thank Eric Williams, NOAA, for SO_2 data. This work was supported by NOAA grants NA100AR4310101 and NA090AR4310122 and DOE SBIR Grant DE-5C0001801. We thank the crew and scientists on the R/V *Atlantis* for their support. Thanks also to Ryan McGovern for instrument assembly and testing.

References

Asaf, D., E. Rotenberg, F. Tatarinov, U. Dicken, S. A. Montzka, and D. Yakir (2013), Ecosystem photosynthesis inferred from measurements of carbonyl sulphide flux, *Nat. Geosci.*, *6*(3), 186–190, doi:10.1038/ngeo1730.

Barnes, I., K. H. Becker, and N. Mihalopoulos (1994), An FTIR product study of the photooxidation of dimethyl disulfide, *J. Atmos. Chem.*, *18*(3), 267–289.

Barnes, I., K. H. Becker, and I. V. Patroescu (1996), FTIR product study of the OH initiated oxidation of dimethyl sulphide: Observation of carbonyl sulphide and dimethyl sulphoxide, *Atmos. Environ.*, *30*, 1805–1814.

Blake, N. J., et al. (2004), Carbonyl sulfide and carbon disulfide: Large-scale distributions over the western Pacific and emissions from Asia during TRACE-P, *J. Geophys. Res. Atmos.*, *109*, D15S05, doi:10.1029/2003JD004259.

Blake, N. J., et al. (2008), Carbonyl sulfide (OCS): Large-scale distributions over North America during INTEX-NA and relationship to CO_2, *J. Geophys. Res. Atmos.*, *113*, D09S90, doi:10.1029/2007JD009163.

Blonquist, J. M., Jr., S. A. Montzka, J. W. Munger, D. Yakir, A. R. Desai, D. Dragoni, T. J. Griffis, R. K. Monson, R. L. Scott, and D. R. Bowling (2011), The potential of carbonyl sulfide as a proxy for gross primary production at flux tower sites, *J. Geophys. Res. Biogeosci.*, *116*, G04019, doi:10.1029/2011JG001723.

Caird, M. A., J. H. Richards, and L. A. Donovan (2006), Nighttime stomatal conductance and transpiration in C3 and C4 plants, *Plant Physiol.*, *143*(1), 4–10, doi:10.1104/pp.106.092940.

Campbell, J. E., et al. (2008), Photosynthetic control of atmospheric carbonyl sulfide during the growing season, *Science*, *322*(5904), 1085–1088, doi:10.1126/science.1164015.

Castro, M. S., and J. N. Galloway (1991), A comparison of sulfur-free and ambient air enclosure techniques for measuring the exchange of reduced sulfur gases between soils and the atmosphere, *J. Geophys. Res. Atmos.*, *96*, 15427–15437, doi:10.1029/91JD01399.

Chin, M., and D. Davis (1995), A reanalysis of carbonyl sulfide as a source of stratospheric background sulfur aerosol, *J. Geophys. Res. Atmos.*, *100*, 8993–9005.

Conrad, R., and K. Meuser (2000), Soils contain more than one activity consuming carbonyl sulfide, *Atmos. Environ.*, *34*(21), 3635–3639.

Daley, M. J., and N. G. Phillips (2006), Interspecific variation in nighttime transpiration and stomatal conductance in a mixed New England deciduous forest, *Tree Physiol.*, *26*(4), 411–419, doi:10.1093/treephys/26.4.411.

Draxler, R. R., and G. D. Rolph (2012), HYSPLIT (Hybrid Single Particle Lagrangian Integrated Trajectory) Model access via NOAA ARL READY Website, ready.arl.noaa.gov.

Faist, J., F. Capasso, D. L. Sivco, C. Sirtori, A. L. Hutchinson, and A. Y. Cho (1994), Quantum Cascade Laser, *Science*, *264*(5158), 553–556, doi:10.1126/science.264.5158.553.

de Gouw, J. A., C. Warneke, S. A. Montzka, J. S. Holloway, D. D. Parrish, F. C. Fehsenfeld, E. L. Atlas, R. J. Weber, and F. M. Flocke (2009), Carbonyl sulfide as an inverse tracer for biogenic organic carbon in gas and aerosol phases, *Geophys. Res. Lett.*, *36*, L05804, doi:10.1029/2008GL036910.

Hines, M. E., R. E. Pelletier, and P. M. Crill (1993), Emissions of sulfur gases from marine and freshwater wetlands of the Florida everglades: Rates and extrapolation using remote sensing, *J. Geophys. Res. Atmos.*, *98*, 8991–8999, doi:10.1029/92JD03019.

Kesselmeier, J., N. Teusch, and U. Kuhn (1999), Controlling variables for the uptake of atmospheric carbonyl sulfide by soil, *J. Geophys. Res. Atmos.*, *104*, 11577–11584.

Kettle, A. J. (2002), Global budget of atmospheric carbonyl sulfide: Temporal and spatial variations of the dominant sources and sinks, *J. Geophys. Res. Atmos.*, *107*(D22), 4658, doi:10.1029/2002JD002187.

Kettle, A., T. Rhee, M. von Hobe, M. Andreae, A. Poulton, and J. Aiken (2001), Assessing the flux of different volatile sulfur gases from the ocean to the atmosphere, *J. Geophys. Res. Atmos.*, *106*, 12193–12209.

Kuhn, U., C. Ammann, A. Wolf, F. Meixner, M. Andreae, and J. Kesselmeier (1999), Carbonyl sulfide exchange on an ecosystem scale: Soil represents a dominant sink for atmospheric COS, *Atmos. Environ.*, *33*(6), 995–1008.

Liu, J., C. Geng, Y. Mu, Y. Zhang, Z. Xu, and H. Wu (2010), Exchange of carbonyl sulfide(COS) between the atmosphere and various soils in China, *Biogeosciences*, *7*(2), 753–762.

McManus, J. B., M. S. Zahniser, D. D. Nelson, J. H. Shorter, S. Herndon, E. Wood, and R. Wehr (2010), Application of quantum cascade lasers to high-precision atmospheric trace gas measurements, *Opt. Eng.*, *49*(11), 111124, doi:10.1117/1.3498782.

McManus, J. B., M. S. Zahniser, and D. D. Nelson (2011), Dual quantum cascade laser trace gas instrument with astigmatic Herriott cell at high pass number, *Appl. Opt.*, *50*(4), A74–A85, doi:10.1364/AO.50.000A74.

Mihalopoulos, N., and B. C. Nguyen (2001), Vertical distribution of carbonyl sulfide in a eucalyptus forest, *Chemosphere: Global Change Sci.*, *3*(3), 275–282, doi:10.1016/S1465-9972(01)00010-1.

Montzka, S., M. Aydin, M. Battle, J. Butler, E. Saltzman, B. Hall, A. Clarke, D. Mondeel, and J. Elkins (2004), A 350-year atmospheric history for carbonyl sulfide inferred from Antarctic firn air and air trapped in ice, *J. Geophys. Res. Atmos.*, *109*, D22302, doi:10.1029/2004JD004686.

Montzka, S. A., P. Calvert, B. D. Hall, J. W. Elkins, T. J. Conway, P. P. Tans, and C. Sweeney (2007), On the global distribution, seasonality, and budget of atmospheric carbonyl sulfide (COS) and some similarities to CO_2, *J. Geophys. Res. Atmos.*, *112*, D09302, doi:10.1029/2006JD007665.

Nelson, D. D., J. B. McManus, S. Urbanski, S. Herndon, and M. S. Zahniser (2004), High precision measurements of atmospheric nitrous oxide and methane using thermoelectrically cooled mid-infrared quantum cascade lasers and detectors, *Spectrochim. Acta A Mol. Biomol. Spectrosc.*, *60*(14), 3325–3335, doi:10.1016/j.saa.2004.01.033.

Protoschill-Krebs, G., C. Wilhelm, and J. Kesselmeier (1996), Consumption of carbonyl sulphide (COS) by higher plant carbonic anhydrase (CA), *Atmos. Environ.*, *30*(18), 3151–3156, doi:10.1016/1352-2310(96)00026-X.

Prueger, J. H., J. L. Hatfield, T. B. Parkin, W. P. Kustas, and T. C. Kaspar (2004), Carbon dioxide dynamics during a growing season in midwestern cropping systems, *Environ. Manage.*, *33*(S1), S330–S343, doi:10.1007/s00267-003-9142-1.

Ryerson, T. B., et al. (2013), The 2010 California research at the nexus of air quality and climate change (CalNex) field study, *J. Geophys. Res. Atmos.*, *118*, 1–37, doi:10.1002/jgrd.50331.

Sandoval-Soto, L., M. Stanimirov, M. von Hobe, V. Schmitt, J. Valdes, A. Wild, and J. Kesselmeier (2005), Global uptake of carbonyl sulfide (COS) by terrestrial vegetation: Estimates corrected by deposition velocities normalized to the uptake of carbon dioxide (CO_2), *Biogeosciences*, *2*(2), 125–132, doi:10.5194/bg-2-125-2005.

Schenk, S., and J. Kesselmeier (2004), How does the exchange of one oxygen atom with sulfur affect the catalytic cycle of carbonic anhydrase?, *Chem. - Eur. J.*, *10*, 3091–3105, doi:10.1002/chem.200305754.

Seibt, U., J. Kesselmeier, L. Sandoval-Soto, U. Kuhn, and J. A. Berry (2010), A kinetic analysis of leaf uptake of COS and its relation to transpiration, photosynthesis and carbon isotope fractionation, *Biogeosciences*, *7*(1), 333–341.

Simmons, J. S., L. Klemedtsson, H. Hultberg, and M. E. Hines (1999), Consumption of atmospheric carbonyl sulfide by coniferous boreal forest soils, *J. Geophys. Res. Atmos.*, *104*, 11569–11576.

Steinbacher, M., H. G. Bingemer, and U. Schmidt (2004), Measurements of the exchange of carbonyl sulfide (OCS) and carbon disulfide (CS_2) between soil and atmosphere in a spruce forest in central Germany, *Atmos. Environ.*, *38*(35), 6043–6052, doi:10.1016/j.atmosenv.2004.06.022.

Stimler, K., D. D. Nelson, and D. Yakir (2009), High precision measurements of atmospheric concentrations and plant exchange rates of carbonyl sulfide using mid-IR quantum cascade laser, *Glob. Chang. Biol.*, *16*, 2496–2503, doi:10.1111/j.1365-2486.2009.02088.x.

Stimler, K., S. A. Montzka, J. A. Berry, Y. Rudich, and D. Yakir (2010), Relationships between carbonyl sulfide (COS) and CO_2 during leaf gas exchange, *New Phytol.*, *186*(4), 869–878, doi:10.1111/j.1469-8137.2010.03218.x.

Stimler, K., J. Berry, and D. Yakir (2012), Effects of carbonyl sulfide and carbonic anhydrase on stomatal conductance, *Plant Physiol.*, *158*, 524–530.

Suntharalingam, P., A. J. Kettle, S. M. Montzka, and D. J. Jacob (2008), Global 3-D model analysis of the seasonal cycle of atmospheric carbonyl sulfide: Implications for terrestrial vegetation uptake, *Geophys. Res. Lett.*, *35*, L19801, doi:10.1029/2008GL034332.

Svoronos, P. D. N., and T. J. Bruno (2002), Carbonyl sulfide: A review of its chemistry and properties, *Ind. Eng. Chem. Res.*, *41*(22), 5321–5336, doi:10.1021/ie020365n.

Van Diest, H., and J. Kesselmeier (2008), Soil atmosphere exchange of carbonyl sulfide (COS) regulated by diffusivity depending on water-filled pore space, *Biogeosciences*, *5*(2), 475–483.

Watts, S. F. (2000), The mass budgets of carbonyl sulfide, dimethyl sulfide, carbon disulfide and hydrogen sulfide, *Atmos. Environ.*, *34*(5), 761–779.

Whelan, M. E., D.-H. Min, and R. C. Rhew (2013), Salt marsh vegetation as a carbonyl sulfide (COS) source to the atmosphere, *Atmos. Environ.*, *73*(C), 131–137, doi:10.1016/j.atmosenv.2013.02.048.

Xu, X., H. G. Bingemer, H. W. Georgii, U. Schmidt, and U. Bartell (2001), Measurements of carbonyl sulfide (COS) in surface seawater and marine air, and estimates of the air-sea flux from observations during two Atlantic cruises, *J. Geophys. Res. Atmos.*, *106*, 3491–3502.

Xu, X., H. G. Bingemer, and U. Schmidt (2002), The flux of carbonyl sulfide and carbon disulfide between the atmosphere and a spruce forest, *Atmos. Chem. Phys.*, *2*, 171–181.

Yi, Z., X. Wang, G. Sheng, D. Zhang, G. Zhou, and J. Fu (2007), Soil uptake of carbonyl sulfide in subtropical forests with different successional stages in south China, *J. Geophys. Res. Atmos.*, *112*, D08302, doi:10.1029/2006JD008048.

Yi, Z., X. Wang, G. Sheng, and J. Fu (2008), Exchange of carbonyl sulfide (OCS) and dimethyl sulfide (DMS) between rice paddy fields and the atmosphere in subtropical China, *Agric. Ecosyst. Environ.*, *123*(1-3), 116–124, doi:10.1016/j.agee.2007.05.011.